

Properties of hydroxyapatite/zirconium oxide nanocomposites

Winatsara Kantana^a, Parkpoom Jarupoom^{a,b}, Kamonpan Pengpat^a, Sukum Eitssayeam^a,
Tawee Tunkasiri^a, Gobwute Rujijanagul^{a,*}

^aDepartment of Physics and Materials Science, Faculty of Science, Chiang Mai University, 50200 Chiang Mai, Thailand

^bDepartment of Industrial Engineering, Faculty of Engineering, Rajamangala University of Technology Lanna, 50300 Chiang Mai, Thailand

Available online 16 October 2012

Abstract

Effects of zirconium oxide (ZrO_2) nanoparticles additive on the microstructure and physical properties of hydroxyapatite (HA) were investigated. The HA powder was derived from natural bovine bone by a sequence of thermal processes. The composites containing nanoparticles of ZrO_2 (0.2–1.0 vol%) were fabricated by a solid-state reaction mixed oxide method. All samples showed traces of HA, beta-tricalcium phosphate (β -TCP) and alpha-tricalcium phosphate (α -TCP) phases while the $x \geq 0.1$ samples also showed ZrO_2 phase. Amount of β -TCP and α -TCP phases tend to decrease with ZrO_2 . The additive inhibited grain growth as a result of a decrease in grain size. However, the $x=0.2$ sample exhibited higher hardness value which is consistent with the density data. In addition, bioactivity test suggested that the additive promoted an apatite forming with the values of Ca/P close to the value obtained from HA.

© 2013 Elsevier Ltd and Techna Group S.r.l. All rights reserved.

Keywords: A. Sintering; D. Apatite; D. ZrO_2 ; E. Biomedical application

1. Introduction

Titanium is widely used for the artificial bone applications, due to its high bio-affinity and favourable mechanical properties [1]. However, according to the recent report, the demand of higher bio-safety materials has been increased for to preventing allergies caused by the elution of Ti ions [2]. Therefore, other material such as hydroxyapatite ($\text{Ca}_{10}(\text{PO}_4)_6(\text{OH})_2$, HA) has been proposed for the applications [3]. Generally, HA is a source material of apatite blocks; the principle component of teeth and bones, and is known for its high bio-affinity [4]. HA has been widely employed for artificial bones due to its excellent biocompatibility and bioactivity with human body [5]. However, the mechanical properties of synthetic HA are low compared to the cortical bone [1]. Therefore, development of bone restorative materials with both higher biocompatibility and sufficient mechanical strength is strongly desired.

To synthesise HA, many approaches have been proposed such as the hydrothermal method [6], continuous

precipitation [2] and the solid state reaction method [4]. However, the costs of raw materials for the preparation, especially for the chemical route are quite high. Further, the yield product that obtained from these methods is so small. Therefore, HA derived from natural sources such as natural calcite and bovine bone have been proposed [7,8]. Further, process for producing HA from natural sources is simple and practical with low cost.

Since the mechanical properties of HA is limited, the incorporation of resistant oxide phase such as zirconia (ZrO_2) has been proposed to optimise biocompatibility and enhance the mechanical properties [9]. ZrO_2 is a well known material which has high mechanical properties and low toxicity [8]. Therefore, it has been used as a biomaterial for dental implants [1], and is expected to be a new bone restorative material.

To our knowledge, nanocomposites of HA and ZrO_2 have not been widely investigated. In the present work, HA/ ZrO_2 nanocomposites were fabricated in various sintering conditions. Raw powder of HA was derived from natural sources, i.e. bovine bone, to achieve the low processing cost. Effects of ZrO_2 nanoparticles on the properties of the composites were investigated.

*Corresponding author. Tel.: +66 5394 3376; fax: +66 533 57512.

E-mail address: rujijanagul@yahoo.com (G. Rujijanagul).

2. Experimental

The hydroxyapatite powder was derived from natural bovine bone via thermal processes. The fresh bones from some parts of a cow were cut into smaller pieces and cleaned well to remove macroscopic adhering impurities. The bone samples were boiled in the distilled water for 8 h for removal of the bone marrow and tendons. After that the bone has been deproteinized by continued boiling in water. The boiled bone samples were then dried over night at a temperature of 200 °C. The deproteinized bone was calcined at 800 °C for 3 h at a heating rate of 100 °C/h and cooling rate of 300 °C/h. The nanoparticles of ZrO₂ (Sigma-Aldrich, 99.8%) were dispersed by ultrasonic in ethanol and added into HA with ratios of 0, 0.2, 0.5, and 1.0 vol %. The ZrO₂/HA mixed powder was uniaxially pressed at 100 MPa into pellets. The compacted green bodies were sintered at the temperatures ranging from 1300–1450 °C for 2 h using a heating rate of 5 °C/min. Density of the sintered samples was determined by using the Archimedes method and distilled water was used as the fluid medium. The phases formation of the sintered samples was analysed by X-ray diffraction technique (XRD). The crystalline phase compositions were identified according to JCPDS data. The mechanical property and hardness values were investigated using a Vickers hardness tester. The microstructural investigation of the samples was performed using a scanning electron microscope (SEM). For bioactivity test the samples were immersed in to a simulated body fluid (SBF) for 7 days. After immersing in SBF, surface samples were studied by SEM and EDS techniques.

3. Result and discussion

The density values of the HA/ZrO₂ composites sintered under various sintering temperatures are shown in Fig. 1. It can be seen that concentration of the additive influenced the sintered density. The density increased with additive content up to 0.2 vol% and then decreased with further

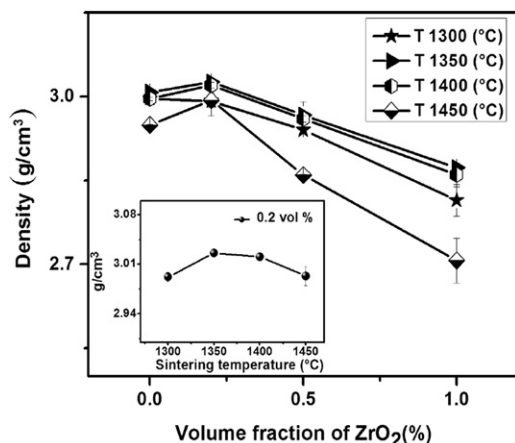


Fig. 1. Density of HA/ZrO₂ composites with various ZrO₂ volume fractions.

concentration, suggesting that the density of the composites could be improved by adding the very small amount of additive. This behaviour can be found in many nanocomposites. In the case of 0.2 vol% samples, the optimum density was observed for the sample sintered at 1350 °C (inset of Fig. 1), indicating that sintering was completed or nearly completed at this temperature. The lower density for higher ZrO₂ content is properly due to the mismatch between the different components leading to an inhibition of the sintering ability.

Fig. 2. shows the XRD patterns of the studied samples. The XRD data revealed that the main phase of all samples is HA. However, beta-tricalcium phosphate (β -TCP) and alpha-tricalcium phosphate (α -TCP) phases were observed as minor phases. These minor phases are often detected in HA ceramics sintered at high temperatures [10]. The presence of β -TCP and α -TCP may be due to the loss of OH⁻ in the structure when HA is heated in air at high temperature. Further, trace of ZrO₂ phase was clearly observed in the XRD patterns for the 0.2–1.0 samples, as expected for these composites. Generally, the formation of small amounts of β -TCP can enhance the bioactivity of materials [11]. Further, the TCP ceramic also shows higher resorbing capacity comparing to the pure HA. Thus, biphasic composites have been fabricated to obtain the optimum properties for biomaterial applications. In addition, many authors reported that α - and β -TCP can be promoted by adding some additives [12,13]. It should be noted that the intensity of α - and β -TCP phases in the present XRD patterns tends to decrease with increasing additive content (inset of Fig. 2). This may be due to the additive inhibited the decomposition of HA. However, further work should be performed to study this effect in detail.

SEM micrographs of the as sintered surfaces of the composites are displayed in Fig. 3. Microstructural analysis revealed that ZrO₂ additions produced a decrease in grain size. Average values of grain size decreased from

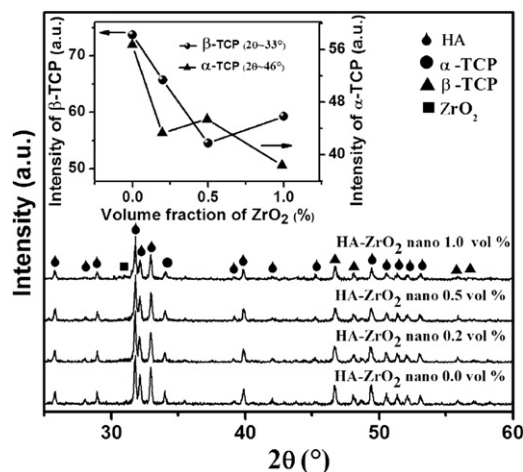


Fig. 2. XRD patterns of HA/ZrO₂ composites sintered at 1350 °C.

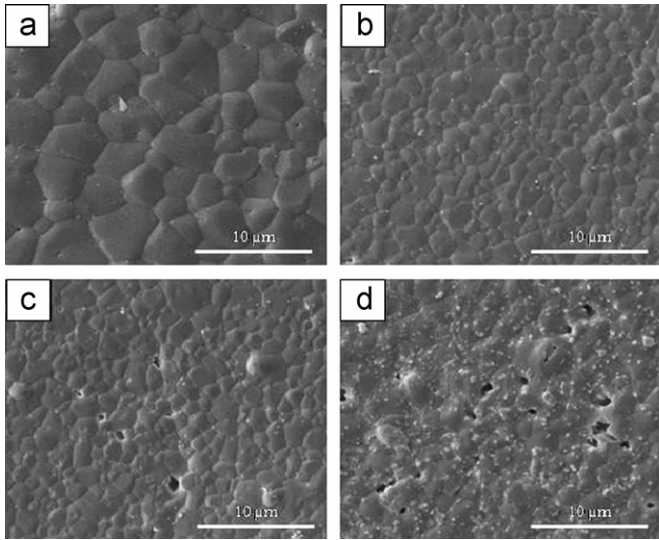


Fig. 3. SEM photographs of the sample surface, containing ZrO_2 for (a) 0.0 vol% (b) 0.2 vol%, (c) 0.5 vol% and (d) 1.0 vol% of ZrO_2 .

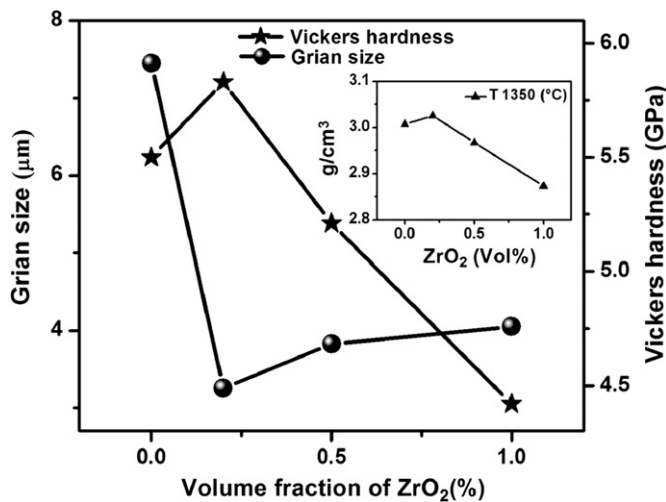


Fig. 4. Grain size and Vickers hardness of HA ceramic and composites at various ZrO_2 contents. Inset shows density of samples (sintered at 1300°C) versus ZrO_2 content.

$\sim 8 \mu\text{m}$ for unmodified HA to $\sim 4 \mu\text{m}$ for the composites, indicating that the additive inhibited grain growth. Further, porosity levels at the sample surfaces were consistent with the density data where the 0.2 vol% sample exhibited the denser surface. It should be noted that the particles of ZrO_2 were clearly observed for the samples contented $\text{ZrO}_2 > 0.2 \text{ vol\%}$. This result is consistent with the XRD examination.

The average values of Vicker hardness for the samples were measured and the value was in the range of 4.8–5.6 GPa. The Vicker hardness of the 0.2 vol% pellets was higher than that of other samples. It should be noted that the hardness data matches well with that of the measured density. Although the enhancement of the hardness value is often related to the reduction of grain size, the

improvement in the mechanical property for the present work is believed to be related to the density or porosity of the samples (inset of Fig. 4).

For bioactivity test, the samples were immersed in SBF. After soaking, microstructure of the sample surface was studied by SEM. Fig. 5. shows SEM micrographs of the sample surfaces sintered at 1350°C samples after immersed in SBF. Apatite particles were observed on the surface of all tested samples. Area of the precipitated apatite increased with increasing ZrO_2 content, indicating that the additive promoted the apatite formation. In the present work, the Ca/P value has been determined by EDS at many areas of the apatite particles.

The average Ca/P value as a function of ZrO_2 content is illustrated in Fig. 6. The Ca/P ratio decreased from 1.88 for the unmodified sample to 1.70 for the 1.0 vol% sample.

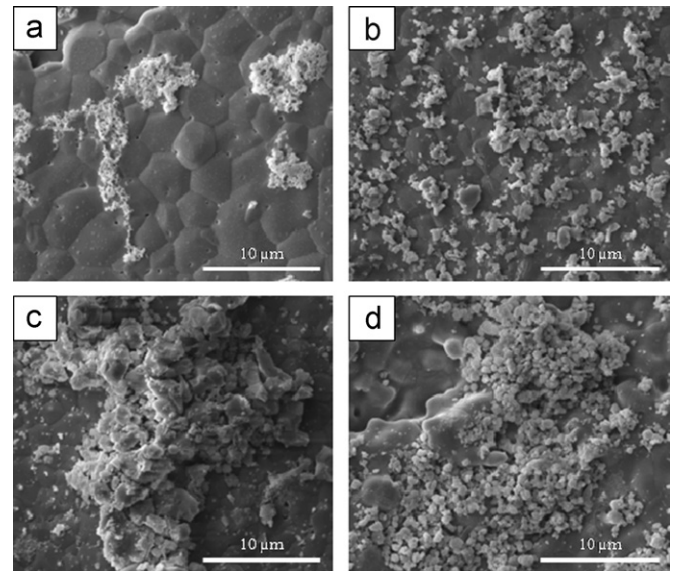


Fig. 5. SEM micrographs of the 1350°C samples after immersing in SBF (a) HA ceramics, (b) HA-0.2 vol% ZrO_2 , (c) HA-0.5 vol% ZrO_2 and (d) HA-1.0 vol% ZrO_2 .

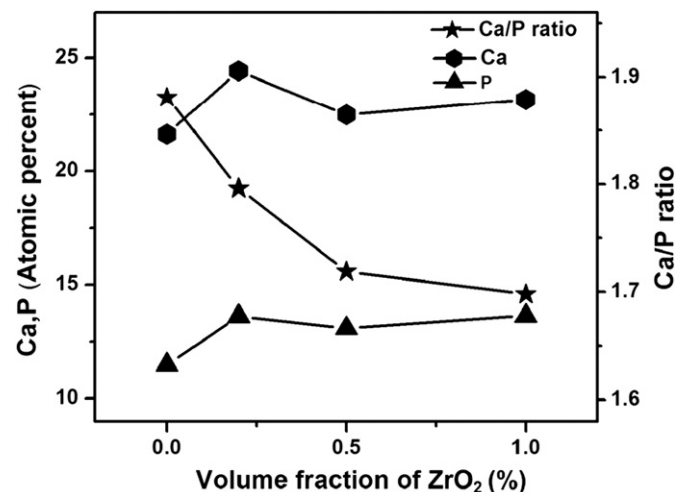


Fig. 6. Ca/P value versus volume fraction of ZrO_2 .

Since the change of Ca/P value is very small, it may be assumed that the additive has slightly affected the Ca/P ratio of the precipitated apatite. In general, pure HA and tetracalcium phosphate show the Ca/P ratio of 1.66 and 2.0, respectively [14]. Therefore, the precipitated apatite particles exhibited a Ca-rich calcium phosphate compound where their composition is close to HA. Kim et al. proposed that the variation in Ca/P ratio of their precipitated apatite could be related with the change in surface charge of HA samples. After soaking the HA samples in SBF for a longer time, however, they found that the Ca/P ratio converged to a value of ~ 1.65 [15]. Therefore, in the present work, the change in Ca/P ratio may be linked to the surface charge of the samples. However, further work is needed to clarify the reason.

4. Conclusions

In this study, properties of HA/ZrO₂ nanocomposites were investigated. XRD examination indicated that the samples consisted of HA, β -TCP, α -TCP and ZrO₂ phases, but β -TCP and α -TCP phases were inhibited and decreased with ZrO₂. Adding the additive resulted in the values of higher density and hardness for the $x=0.2$ sample, but it resulted in the decrease in grain size. The additive also helps the apatite formation after soaking in the SBF. However, further work should be performed to understand the mechanism of apatite forming in the nanocomposites.

Acknowledgements

This work was supported by the Office of the Higher Education Commission (OHEC), National Research Council of Thailand, Hands-on Research and Development Project; Rajamangala University of Technology Lanna and the Faculty of Science and the Graduate School of Chiang Mai University.

References

- [1] H. Egusa, N. Ko, T. Shimazu, H. Yatani, Suspected association of an allergic reaction with titanium dental implants: a clinical report, *Journal of Prosthetic Dentistry* 100 (2008) 344–347.
- [2] D. Shi, G. Jiang, X. Wen, J. Biomed, In vitro bioactive behavior of hydroxyapatite-coated porous Al₂O₃, *Journal of Biomedical Materials Research* 53 (2000) 457–466.
- [3] L.L. Hench, J. Wilson, Surface-active biomaterials, *Science* 226 (1984) 630–636.
- [4] S. Pramanik, A.K. Agarwaly, K.N. Rai, Development of high strength hydroxyapatite for hard tissue replacement, *Trends in Biomaterials and Artificial Organs* 19 (2005) 46–51.
- [5] J. Raveh, H. Stich, F. Sutter, R. Greiner, Use of the titanium-coated hollow screw and reconstruction plate system in bridging of lower jaw defects, *Journal of Maxillofacial and Oral Surgery* 42 (1984) 281–294.
- [6] N. Kivrak, A.C. Tas, Synthesis of calcium hydroxyapatite–tricalcium phosphate (HA–TCP) composite bioceramic powders and their sintering behavior, *Journal of the American Ceramic Society* 81 (1998) 2245–2252.
- [7] M.K. Herliansyah, D.A. Nasution, M. Hamdi, A. Ide-Ektessabi, M.W. Wildan, A.E. Tontowi, Preparation and characterization of natural hydroxyapatite: a comparative study of bovine bone hydroxyapatite and hydroxyapatite from calcite, *Materials Science Forum* 561–565 (2007) 1441–1444.
- [8] C.Y. Ooi, M. Hamdi, S. Ramesh, Properties of hydroxyapatite produced by annealing of bovine bone, *Ceramics International* 33 (2007) 1171–1177.
- [9] V.V. Silva, F.S. Lameiras, Synthesis and characterization of composite powders of partially stabilized zirconia and hydroxyapatite, *Materials Characterization* 45 (2000) 51–59.
- [10] A. Raksujarit, K. Pengpat, G. Rujijanagul, T. Tunkasiri, Processing and properties of nanoporous hydroxyapatite ceramics, *Materials and Design* 31 (2010) 1658–1660.
- [11] S.J. Kalita, S. Bose, H.L. Hosick, A. Bandyopadhyay, CaO–P₂O₅–Na₂O-based sintering additives for hydroxyapatite (HAp) ceramics, *Biomaterials* 25 (2004) 2331–2339.
- [12] D.C. Tancred, B.A.O. McCormack, A.J. Carr, A quantitative study of the sintering and mechanical properties of hydroxyapatite/phosphate glass composites, *Biomaterials* 19 (1998) 1735–1743.
- [13] S. Ramesh, C.Y. Tan, W.H. Yeo, R. Tolouei, M. Amiryan, I. Sopyan, W.D. Teng, Effects of bismuth oxide on the sinterability of hydroxyapatite, *Ceramics International* 37 (2011) 599–606.
- [14] W. Suchanek, M. Yoshimura, Processing and properties of hydroxyapatite-based biomaterials for use as hard tissue replacement implants, *Journal of Biomedical Materials Research* 13 (1998) 94–117.
- [15] H.M. Kim, T. Himeno, T. Kokubo, T. Nakamura, Process and kinetics of bonelike apatite formation on sintered hydroxyapatite in a simulated body fluid, *Biomaterials* 26 (2005) 4366–4373.